see commentary on page 555

Autophagy is cytoprotective during cisplatin injury of renal proximal tubular cells

Sudharsan Periyasamy-Thandavan[1], Man Jiang[1], Qingqing Wei[1], Robert Smith[1], Xiao-Ming Yin[3] and Zheng Dong[1,2]

[1]*Department of Cellular Biology and Anatomy, Medical College of Georgia, Augusta, Georgia, USA;* [2]*Charlie Norwood VA Medical Center, Augusta, Georgia, USA and* [3]*Department of Pathology, University of Pittsburgh, Pittsburgh, Philadelphia, USA*

Autophagy is a cellular process of bulk degradation of damaged organelles, protein aggregates and other macromolecules in the cytoplasm. It is thought to be a general response to stress contributing to cell death; alternatively it might act as a cytoprotective mechanism. Here we found that administration of cisplatin induced the formation of autophagic vesicles and autophagosomes in mouse kidneys. In cultured proximal tubular cells, the nephrotoxin caused autophagy in a dose- and time-dependent manner prior to apoptosis. Notably, autophagy occurred within hours of cisplatin administration but this was partially suppressed by the p53 inhibitor pifithrin-α, suggesting that p53 is involved in autophagic signaling. This cisplatin-induced autophagy was attenuated in renal cells stably transfected with Bcl-2, suggesting an anti-autophagic role for this well-known anti-apoptotic protein. Blockade of autophagy with pharmacological inhibitors (3-methyladenine or bafilomycin) or shRNA knockdown of the autophagic gene Beclin increased tubular cell apoptosis during cisplatin treatment. Our study has found that autophagy occurs in acute kidney injury and this may be an important protective mechanism for cell survival.

Kidney International (2008) **74,** 631–640; doi:10.1038/ki.2008.214; published online 28 May 2008

KEYWORDS: autophagy; apoptosis; cisplatin; p53; Bcl-2; acute kidney injury

Correspondence: *Zheng Dong, Department of Cellular Biology and Anatomy, Medical College of Georgia, 1459 Laney Walker Blvd, Augusta, Georgia 30912, USA. E-mail: zdong@mail.mcg.edu*

Received 29 November 2007; revised 22 February 2008; accepted 26 March 2008; published online 28 May 2008

Autophagy is a process of bulk degradation of damaged organelles, protein aggregates, and other macromolecules in the cytoplasm.[1–4] At the core of autophagy is a specific family of genes or proteins called autophagy-related gene (Atg). The Atg proteins are responsible for initiation, formation, and maturation of autophagosomes, which subsequently fuses with lysosomes for hydrolysis or degradation of enwrapped materials.[1–4] Atgs were originally identified in yeast, but their mammalian orthologs are now being discovered and shown to play critical roles in autophagy in mammalian cells and animals.[1–4] For example, Beclin-1, the mammalian ortholog of yeast Atg6, contributes to vesicle nucleation, an early event for autophagosome formation.[5] LC3, the mammalian ortholog of Atg8, is proteolytically processed and conjugated with phosphotidylethanolamine to form LC3-II, which is then localized on the autophagic vesicle for its elongation and expansion.[6]

Traditionally, autophagy is recognized as a cellular response to nutrient deprivation or starvation, whereby cells digest a portion of cytoplasm to recycle nutrients for survival. However, recent studies have suggested that autophagy might be a general cellular response to stress.[1–4] Depending on the experimental conditions, autophagy can directly induce cell death or act as a mechanism of cytoprotection. Despite recent rapid progress in autophagy research, very little is known about autophagy in renal cells, tissues or systems.

Acute kidney injury by ischemia, sepsis, or nephrotoxins is a typical condition of renal stress, leading to cell death, tissue damage, and loss of renal function or renal failure.[7–11] Is autophagy induced during acute kidney injury? Does autophagy contribute to renal cell injury and death, or survival under this pathological condition? This study was designed to address these questions by using experimental models of cisplatin nephrotoxicity. Cisplatin is a widely used chemotherapy drug, with major side effects in kidneys, inducing acute kidney injury.[12,13] While multiple mechanisms have been documented to contribute to cisplatin nephrotoxicity,[14–33] how these signaling pathways are integrated to induce renal pathology is largely unknown.[13] Here we demonstrate early occurrence of autophagy during cisplatin treatment of renal tubular cells and tissues.

Importantly, autophagy appears to be a cytoprotective mechanism for cell survival.

RESULTS

Autophagy is induced early during cisplatin treatment, prior to tubular cell apoptosis and renal injury

To determine the occurrence of autophagy during cisplatin nephrotoxicity, we examined an *in vitro* model of cultured proximal tubular cells (RPTC). This model has been characterized in previous studies.[16–18] Our initial analysis was focused on subcellular localization and redistribution of LC3, because redistribution of LC3 from cytosol to a punctate autophagosome staining is an indication of autophagy.[34] To this end, cells were transfected with a green fluorescent protein (GFP)-LC3 fusion plasmid and then treated with 20 μM cisplatin for 0–16 h, followed by examination by fluorescence microscopy. In the control group, 27% of transfected (GFP-labeled) cells had punctate LC3 staining. Six hours of cisplatin treatment increased the percentage of LC3 punctate cells to ~50% (Figure 1a). Further incubation with cisplatin to 12 or 16 h led to gradual disappearance of LC3 puncta, an observation that was consistent with the degradation of LC3 in matured autophagosomes (Figure 1a). Representative LC3 staining in control and cisplatin-treated cells is shown in Figure 1b. By analyzing LC3 redistribution, we further showed that induction of autophagy was dependent on cisplatin dose (Figure 1b). Significant increases of autophagic (LC3 punctate) cells were induced by 5–20 μM, but not 1 or 2 μM, cisplatin (Figure 1c). To further analyze autophagy, we examined formation of LC3-II, the autophagic form of LC3.[35] RPTCs were incubated with 20 μM cisplatin for 0–16 h to collect whole-cell lysates for immunoblot analysis. As shown in Figure 1d, cisplatin induced an obvious accumulation of LC3. Of note, LC3-II, the autophagic form, showed highest accumulation at 6 h of cisplatin treatment and then decreased toward basal levels (Figure 1d), which correlated with the time course of punctate LC3 formation (Figure 1a). As shown in our previous work,[16–18] cisplatin at 20 μM induced significant amounts of apoptosis in RPTCs in a time-dependent manner (Figure 1e). It is noteworthy that occurrence of autophagy was hours earlier than apoptosis (Figures 1a and e). The results suggest that cisplatin-induced autophagy is not caused by or secondary to apoptosis.

We further verified cisplatin-induced autophagy in RPTCs by electron microscopy. As shown by representative micrographs, autophagosomes with characteristic double or multiple membranes were identified in the cells after 6 h of cisplatin treatment (Figure 2a, arrows). In addition, there were many autophagic vacuoles or vesicles (Figure 2a, arrowheads). Counting autophagic vesicles in the micrographs also indicated higher autophagy in cisplatin-treated cells (Figure 2b). Interestingly, these cells also showed autophagic vesicles at different stages of autophagosome apparently from initiation, elongation, complete assembly, to maturation (Figure 2c–g).

Autophagy during cisplatin nephrotoxicity in C57BL/6 mice

To gain initial evidence for autophagy during cisplatin nephrotoxicity *in vivo*, C57BL/6 mice were injected with a single dose of 30 mg/kg cisplatin.[28,36,37] We first examined autophagy by electron microscopy. As shown in Figure 3a, 2 days after cisplatin injection, numerous vacuoles appeared in some proximal tubular cells and some of the vacuoles contained cytosolic materials, becoming autophagic vesicles (arrow). At day 3, the numbers of empty vacuoles decreased, but their sizes increased. In addition, more vesicles had taken up cytosolic materials to become autophagosomes (arrow). Counting cells containing autophagic vacuoles or vesicles showed progressive increase of autophagy during cisplatin nephrotoxicity (Figure 3b). By the end of 2–3 days of cisplatin treatment, over 30% of renal tubular cells were autophagic. To further confirm autophagy, we collected renal tissue lysates for immunoblot analysis of LC3. As shown in Figure 3c, there was a notable increase of LC3-II in renal tissues following cisplatin injection, particularly at day 2 and 3. Together, these results have demonstrated evidence for the occurrence of autophagy during cisplatin-induced renal cell injury.

Effects of p53 inhibition on cisplatin-induced autophagy

We and others have demonstrated a role for p53 in cisplatin-induced renal cell apoptosis *in vitro* and nephrotoxicity *in vivo*.[13,15,17,18,24,36,38] Interestingly, a recent study by Feng *et al.*[39] suggests that p53 may also be involved in the regulation of autophagy. We, therefore, tested the effects of pifithrin-α (PF), a pharmacological inhibitor of p53, on cisplatin-induced autophagy in RPTCs. For this purpose, cells were transfected with GFP-LC3 and then incubated with 20 μM cisplatin in the presence of 20 μM PF. As shown in Figure 4a, cisplatin incubation for 6 h induced punctate GFP-LC3 in 56% of the cells, which was suppressed to 36% by PF. In addition, PF induced an interesting distribution pattern of punctate LC-GFP in the autophagic cells. As shown in Figure 4b, the autophagic cells in the cisplatin + PF group had many big empty vacuoles surrounded by punctate GFP-LC3 staining. We further collected cell lysates for immunoblot analysis of LC3 (Figure 4c). Consistently, PF had partial inhibitory effects on LC3-II formation during cisplatin treatment (Figure 4c and d). Together, these results suggest the involvement of p53 in triggering autophagy during cisplatin treatment of renal tubular cells.

Effects of Bcl-2 on cisplatin-induced autophagy

Bcl-2 is well known for its antiapoptotic activity. Interestingly, recent studies have shown that Bcl-2 is also an anti-autophagic protein,[40] which binds and sequesters Beclin-1 to prevent vesicle nucleation, an early step of autophagosome formation. To determine the regulation of cisplatin-induced autophagy by Bcl-2, we used an RPTC line stably transfected with Bcl-2 that was established in our previous work.[41] Wild-type RPTCs and Bcl-2-transfected cells were incubated with

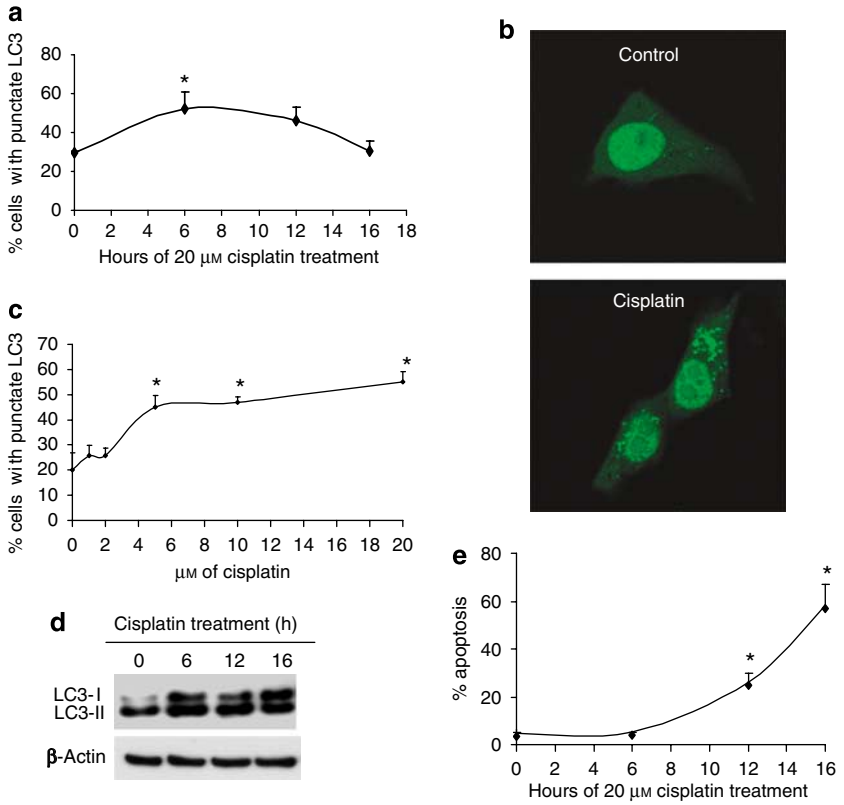

Figure 1 | Cisplatin-induced autophagy in renal proximal tubular cells. (**a**) The time course of cisplatin-induced LC3 punctate formation. RPTCs transiently transfected with GFP-LC3 were incubated with 20 μM cisplatin for 0–16 h. The percentage of cells with punctate GFP-LC3 staining was determined by fluorescence microscopy. (**b**) Representative cell images showing punctate GFP-LC3 distribution after cisplatin treatment. RPTCs transiently transfected with GFP-LC3 were incubated with or without 20 μM cisplatin for 6 h and then examined by confocal microscopy. (**c**) Dose dependence of cisplatin-induced punctate LC3 staining. RPTCs transiently transfected with GFP-LC3 were incubated with 0–20 μM cisplatin for 6 h and then examined by fluorescence microscopy to determine the percentage of cells with punctate GFP-LC3 staining. (**d**) LC3-II formation during cisplatin treatment. RPTCs were incubated with 20 μM cisplatin for 0–16 h to collect whole-cell lysates for immunoblot analysis of LC3 and also β-actin as a protein loading control. (**e**) The time course of cisplatin-induced apoptosis. Apoptosis was assessed by morphological methods. Data in (**a**, **c**, **e**) are expressed as mean ± s.d. ($n = 4$); *, statistically significantly different from the control group without cisplatin treatment. Data in panels **b** and **d** are representative of at least four separate experiments. The results show that cisplatin dose and time dependently induced autophagy, prior to occurrence of apoptosis.

20 μM cisplatin for 6 h. In wild-type RPTCs, cisplatin treatment increased autophagic cells to 57%, while no increase was shown in Bcl-2 cells (Figure 5a). Examination of GFP-LC3 signal at later time points did not reveal significant amounts of autophagic cells in the Bcl-2 group either (Figure 5b). We further analyzed LC3 by immunoblots. Consistent with earlier results (Figure 1), cisplatin induced LC3-II with a maximal accumulation at 6 h; such induction was not shown in Bcl-2 cells (Figure 5c and d). Together, the results demonstrate an impressive inhibitory effects of Bcl-2 on cisplatin-induced autophagy.

Effects of 3-methyladenine and bafilomycin on autophagy during cisplatin treatment

Depending on the experimental conditions, autophagy can be cell killing or cytoprotective.[2,42] What is the pathophysiological role of autophagy during cisplatin-induced tubular cell injury? To address this question, we determined the effects of 3-methyladenine (3-MA) and bafilomycin (BAF), two pharmacological inhibitors of autophagy. We first verified their effects on autophagy. As shown in Figures 6a, 3-MA blocked GFP-LC3 redistribution into punctate form. In stark contrast, BAF enhanced formation of punctate LC3. The results were further supported by cell count (Figure 6b). The opposite effects of 3-MA and BAF on LC3 distribution are not surprising, as these two inhibitors block autophagy at different levels: while 3-MA inhibits the initiation of autophagosome, BAF attenuates fusion of autophagosome with lysosome.[42] As a result, 3-MA blocked autophagosome formation from the beginning, whereas BAF prevented degradation of GFP-LC3 in autophagolysosomes and in turn increased LC3 punctate. This notion was also supported by our immunoblot analysis of LC3 (Figure 6c and d). 3-MA blocked the formation LC3-II in cisplatin-treated as well as in control cells, while BAF preserved LC3-II during cisplatin treatment even at 24 h.

3-MA and BAF enhance apoptosis during cisplatin treatment

After confirming the effects of 3-MA and BAF on autophagy, we examined their effects on apoptosis during cisplatin

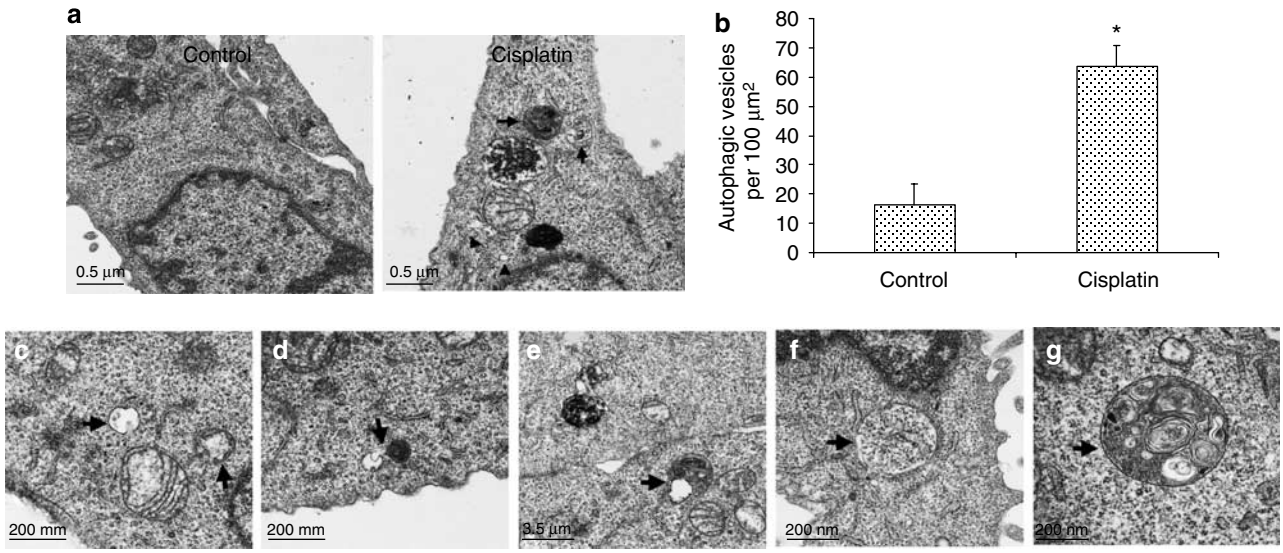

Figure 2 | Electron microscopic analysis of autophagy. RPTCs were incubated with or without 20 μM cisplatin for 6 h. The cells were then fixed and processed for electron microscopy. (**a**) Representative electron micrographs showing autophagosomes and autophagic vesicles in cisplatin-treated cells. Arrows, autophagosomes; arrowheads, autophagic vesicles. (**b**) Quantification of autophagic vesicles. The number of autophagic vesicles per 100 μm^2 was determined in electron micrographs. Data are expressed as means ± s.d. ($n = 4$); *, statistically significantly different from the control cells. (**c–g**) Selected micrographs showing the assembly and progression of autophagic vesicles. (**c**) sequestration of cytoplasm by pre-autophagasome; (**d**) close contact of autophagosome with lysosome; (**e**) docking and fusion of autophagosome with lysosome; (**f**) typical autophagosome containing cytosol; (**g**) typical autophagosome containing organelles.

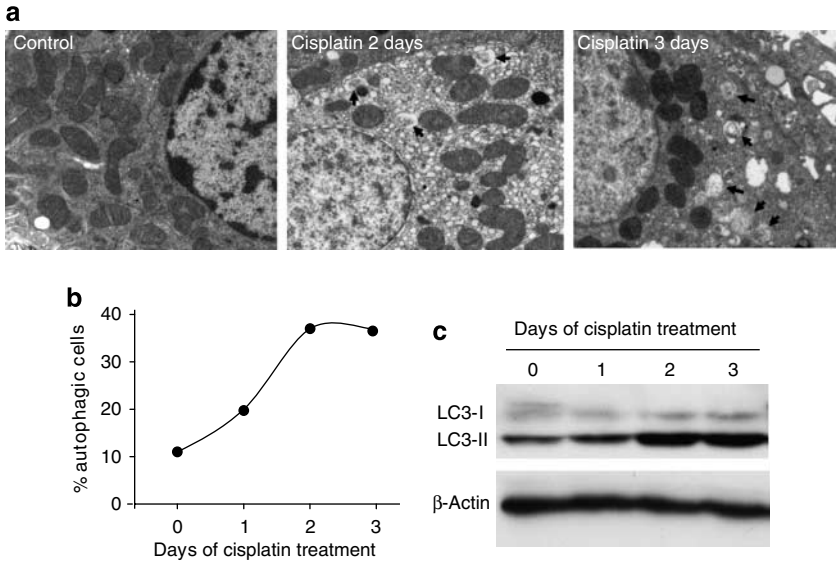

Figure 3 | Autophagy in renal tissues during cisplatin nephrotoxicity *in vivo*. C57BL/6 mice (male, 8–10 weeks old) were injected with 30 mg/kg cisplatin. At the indicated time points, renal cortical tissues were collected for electron microscopy or homogenized for immunoblot analysis of LC3. (**a**) Electron micrograph of representative cells. (**b**) Quantification of tubular cells with autophagic vacuoles or vesicles. Autophagic cells were identified by the presence of numerous autophagic vacuoles, vesicles, or autophagosomes. Over 100 proximal tubular cells from 2–3 animals were evaluated for each time point. (**c**) Immunoblot of LC3. Shown are representative blots of four separate experiments.

treatment. Apoptosis was evaluated based on cellular and nuclear morphology. As shown in Figure 7a, control cells without cisplatin exposure appeared healthy. Incubation with 20 μM cisplatin for 12 h induced apoptosis in some cells, which had a shrunken cell body with condensed and fragmented nuclei. Many of these cells also showed formation of apoptotic bodies or blebs. Importantly, addition of either 3-MA or BAF significantly increased apoptosis during cisplatin incubation (Figure 7). Quantification by cell count indicated that 3-MA and BAF increased apoptosis

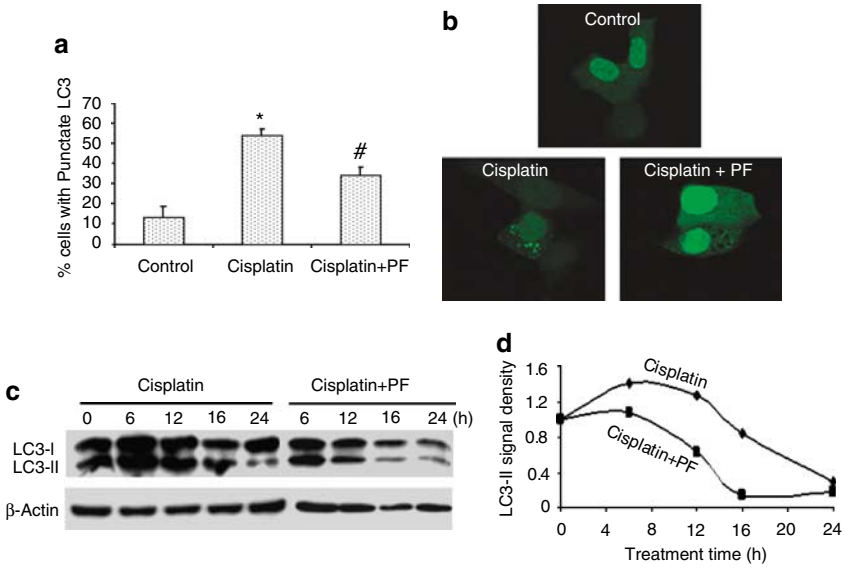

Figure 4 | Effects of PF on cisplatin-induced autophagy. RPTCs transiently transfected with GFP-LC3 were incubated for 6 h with 20 μM cisplatin in the absence or presence of 20 μM PF. (**a**) Percentage of cells with punctate GFP-LC3 pattern. Data are expressed as means ± s.d. ($n = 4$); *, statistically significantly different from the control group; #, significantly different from the cisplatin-only group. (**b**) Representative images of GFP-LC3 distribution in control, cisplatin-treated, and cisplatin + PF-treated cells. (**c**) Immunoblot analysis of LC3-II accumulation. The blots are representative of at least three separate experiments. (**d**) Densitometry of LC3-II signals in immunoblots. The results show that cisplatin-induced autophagy was partially suppressed by PF, a p53 inhibitor.

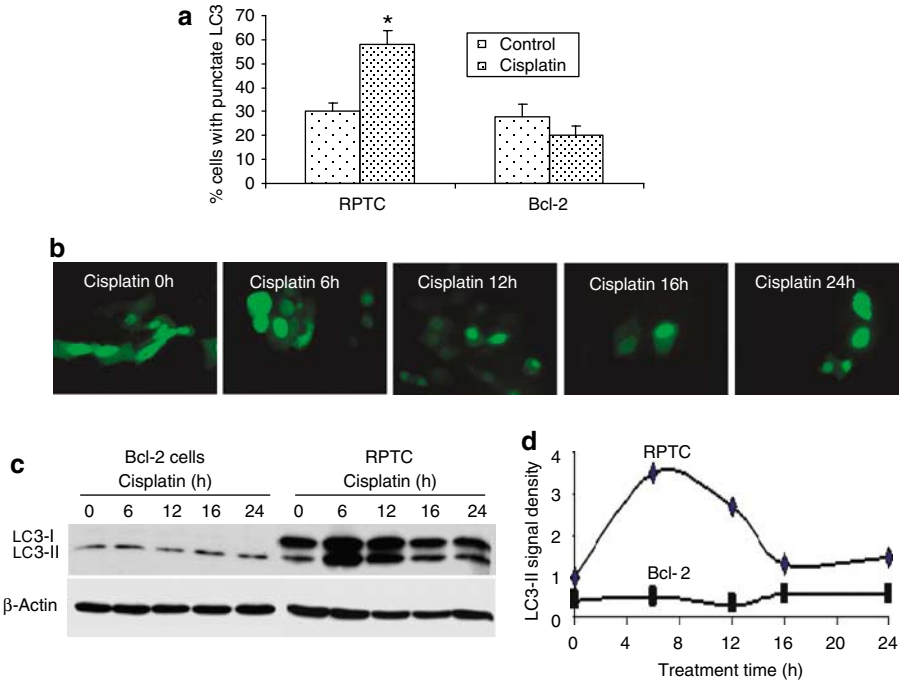

Figure 5 | Effects of Bcl-2 expression on cisplatin-induced autophagy. Wild type and Bcl-2-transfected RPTCs were analyzed in parallel. (**a**) Cisplatin-induced punctate GFP-LC3 distribution. The cells were transiently transfected with GFP-LC3, and incubated with 20 μM cisplatin for 6 h for microscopic evaluation. (**b**) Representative images of GFP-LC3 distributions in Bcl-2 cells during cisplatin treatment. (**c**) Immunoblot analysis of LC3 accumulation. The blots were then reprobed for β-actin to monitor protein loading and transferring. (**d**) Densitometry of LC3-II signals in immunoblots. Data in panel **a** are expressed as mean ± s.d. ($n = 4$); *, statistically significantly different from the control group without cisplatin treatment. Data in panels **b**–**d** are representative of at least three separate experiments. The results show that cisplatin-induced autophagy was diminished by Bcl-2 expression.

from 27% to 47 and 55%, respectively (Figure 7b). We further examined the effects of 3-MA on apoptosis induced by lower concentrations of cisplatin. As shown in Figure 7c, 5 μM cisplatin incubation for 16 h induced ~3% apoptosis, which was increased to ~20% by 3-MA. Together, the pharmacological results suggest that autophagy might be a

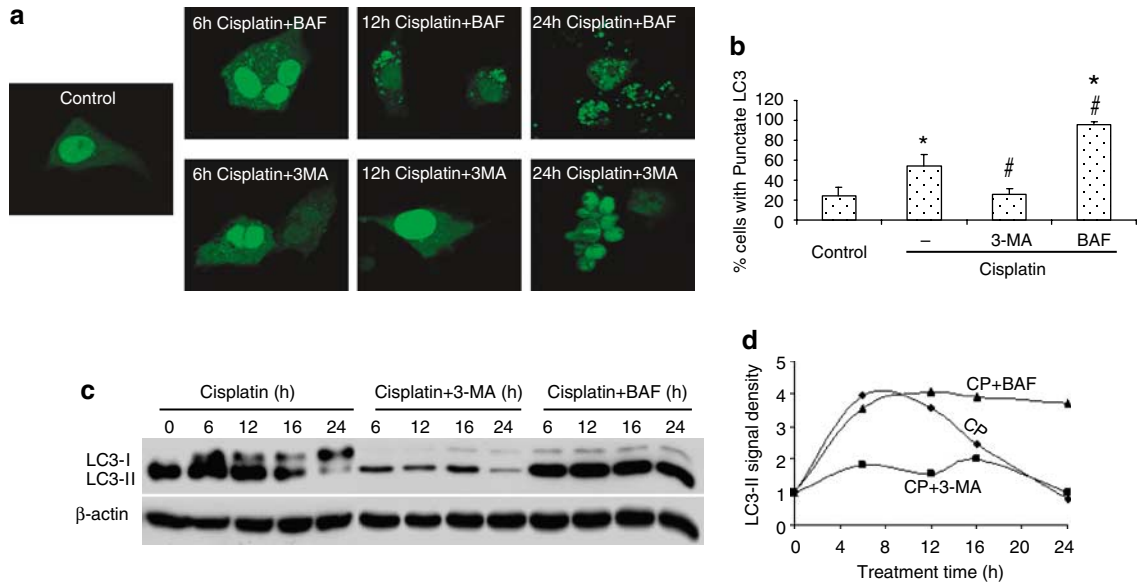

Figure 6 | Effects of 3-MA and BAF on autophagy during cisplatin treatment. RPTCs transiently transfected with GFP-LC3 were cultured for 0–24 h with 20 μM cisplatin in the absence or presence of 100 nm BAF or 10 mM 3-MA. (**a**) Representative images of GFP-LC3 staining in cells treated with cisplatin + BAF or cisplatin + 3-MA. (**b**) Effects of BAF and 3-MA on punctate GFP-LC3 staining. (**c**) Immunoblot analysis of LC3. (**d**) Densitometry of LC3-II signals in immunoblots. Data in **b** are expressed as mean ± s.d. ($n = 4$). *, statistically significantly different from the control group without cisplatin treatment; #, significantly different from the cisplatin-only group. Data in panels **a** and **c** are representative of at least three separate experiments.

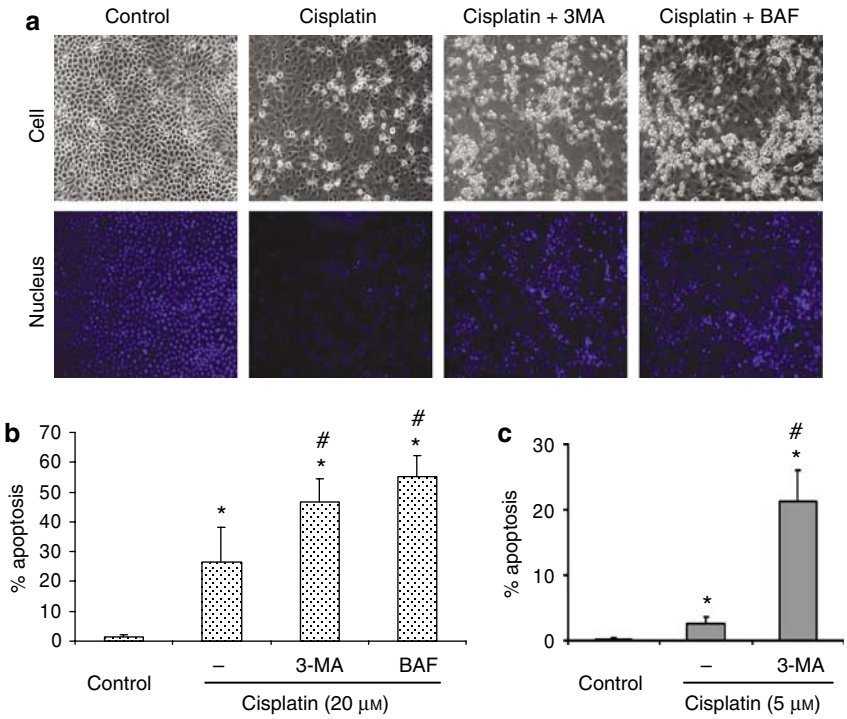

Figure 7 | Pharmacological inhibition of autophagy increases apoptosis during cisplatin treatment. RPTCs were incubated for 12 h with 20 μM cisplatin in the absence or presence of 100 nm BAF or 10 mM 3-MA. The cells were stained with Hoechst 33342 to examine cell and nuclear morphology to analyze apoptosis. (**a**) Representative images of cell morphology and nuclear staining of the same field of cells. (**b**) Percentage of cells showing typical apoptotic morphology. (**c**) RPTCs were incubated with 5 μM cisplatin for 16 h in the absence or presence of 10 mM 3-MA. The percentage of apoptosis was assessed morphologically after treatment. Data in panels **b** and **c** are means ± s.d. of four separate experiments; *, significantly different from the untreated group; #, significantly different from the cisplatin-only treated group. Representative data are expressed as mean ± s.d. ($n = 4$); *, statistically significantly different from the control group without cisplatin treatment; #, significantly different from the cisplatin-only group.

cytoprotective mechanism against apoptosis during cisplatin treatment.

Knockdown of Beclin-1 sensitizes cells to cisplatin-induced apoptosis

To further determine the role of autophagy in cell death or survival during cisplatin treatment, we used short-hairpin RNA (shRNA) to knock down Beclin-1, a critical protein involved in initial autophagic vesicle formation.[5,42] The transfection efficacy was relatively low for RPTCs; thus, human embryonic kidney (HEK) cells were initially used for the shRNA study. Four Beclin-1 shRNAs and one non-targeting control shRNA was first tested for their effects on Beclin-1 expression. As shown in Figure 8a, both #3 and #4 Beclin shRNA significantly attenuated Beclin-1 expression. We then examined the effects of Beclin shRNA#4 on cisplatin-induced autophagy. As expected, transfection with #4, but not the non-targeting control shRNA, blocked autophagic GFP-LC3 distribution during cisplatin treatment (Figure 8b). Importantly, Beclin shRNA sensitized the cells to cisplatin-induced apoptosis. As shown in Figure 8c, cisplatin induced 20% apoptosis, which was increased to 53% by shRNA knockdown of Beclin-1. As a control, the non-targeting shRNA did not have significant effects. We further examined the effects of Beclin knockdown in RPTCs. The shRNA constructs used in our study also had GFP sequence and expressed the fluorescent protein. Thus, RPTCs were transfected with control or Beclin shRNA and then treated with cisplatin. The transfected cells with GFP were specifically analyzed for apoptosis. The results are shown in Figure 8d. While the group transfected with control shRNA had 32% apoptosis, the cells transfected with Beclin shRNA had 52%. Together with the pharmacological results of 3-MA and BAF, the shRNA study has provided strong evidence that autophagy during cisplatin-induced renal injury is an important mechanism for cytoprotection and cell survival.

DISCUSSION

Autophagy has been intensely studied during the past a few years.[1–4] Over 30 Atg genes have been discovered in yeast and their mammalian orthologs are being identified. Importantly, it is now becoming clear that autophagy is a general cellular response to stress, not limited only to nutrient deprivation or starvation. Intriguingly, autophagy can be cell killing or cytoprotective, although it is largely unknown what determine the final outcomes.[2,42] Despite the rapid progress in autophagy research, very little is known about autophagy, its regulation, and pathophysiological role(s) in kidney cells and tissues. This study has demonstrated compelling evidence for the occurrence of autophagy in an experimental model of renal injury. Importantly, we show that autophagy is a cytoprotective mechanism for cell survival under the pathogenic conditions.

The majority of experiments in this study were conducted in an *in vitro* model, where cultured renal proximal tubular cells were incubated with cisplatin to induce cell stress, injury, and death. This model has been used and characterized in our previous studies.[16–18,43] This study has demonstrated the

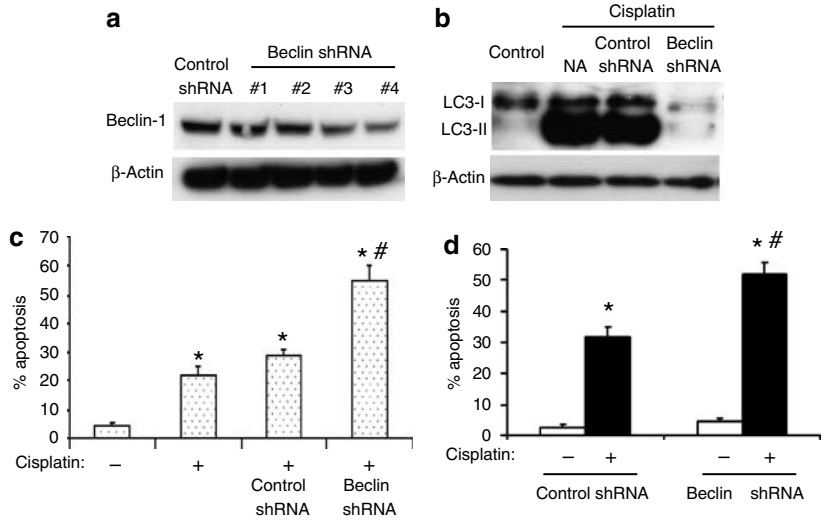

Figure 8 | shRNA knockdown of Beclin-1 sensitizes cells to cisplatin-induced apoptosis. (**a**) shRNA knockdown of Beclin-1. HEK cells were transfected with Beclin-1 shRNA or non-targeting control shRNA for 24 h to collect whole-cell lysates for immunoblot analysis of Beclin-1. (**b**) Effects of Beclin-1 knockdown on cisplatin-induced autophagic LC3-II accumulation. HEK cells transfected with Beclin-1 shRNA (#4) or control shRNA were treated with 40 μM cisplatin for 12 h to collect lysate for immunoblot analysis of LC3. (**c**) Effects of Beclin-1 knockdown on cisplatin-induced apoptosis in HEK cells. HEK cells transfected with Beclin-1 shRNA (#4) or control shRNA were treated with 40 μM cisplatin for 12 h. Apoptosis was analyzed by cell and nuclear morphology. (**d**) Effects of Beclin-1 knockdown on cisplatin-induced apoptosis in HEK cells. RPTCs were transiently transfected with GFP-tagged negative control shRNA or Beclin-1 shRNA. The transfected cells were then untreated or treated with 20 μM cisplatin for 16 h. Apoptosis in transfected (GFP-labeled) cells were determined by cell and nuclear morphology. Data in panels **c** and **d** are expressed as mean ± s.d. ($n = 4$); *, statistically significantly different from the control group without cisplatin treatment; #, significantly different from the cisplatin-only group (NA, no addition of shRNA).

occurrence of autophagy in this model by using multiple techniques, including examination of autophagic or punctate GFP-LC3, immunoblot analysis of LC3-II formation, and electron microscopic detection of autophagosomes. Compared with these cell culture results, the *in vivo* evidence of autophagy is limited, due to technical difficulties of *in vivo* analysis. Nevertheless, by electron microscopy we have demonstrated an increase of autophagic cells during cisplatin nephrotoxicity in C57BL/6 mice. In addition, we have shown accumulation of LC3-II, the autophagic form of LC3, in renal tissues during *in vivo* cisplatin nephrotoxicity (Figure 3).

In the *in vitro* model, we show that autophagy occurs within hours of cisplatin incubation, whereas significant apoptosis is not induced until 12 h (Figure 1). The earlier occurrence of autophagy suggests that it is not caused by, or secondary to, apoptosis. Then, does autophagy contribute to later development of apoptosis in the model system? The answer is, No. As a matter of fact, inhibition of autophagy by using pharmacological and gene-knockdown approaches enhances apoptosis (Figures 7 and 8), suggesting that autophagy during cisplatin treatment is not a cell killing, but a pro-survival, mechanism. Examination of the dose dependence of cisplatin-induced autophagy indicates that autophagy is induced by 5 μM cisplatin (Figure 1b), a concentration that does not induce significant apoptosis in RPTCs (Figure 7c). Thus, in this model, occurrence of autophagy and apoptosis depends on the severity of the injury or stress: autophagy can be induced by mild to moderate stress, whereas apoptosis requires more severe stress.

Mechanistically, we show that cisplatin-induced autophagy is partially inhibited by PF, suggesting a role for p53 in autophagy under the experimental condition. Our previous work has shown that p53 is activated early during cisplatin treatment of RPTCs.[16,17] p53 Phosphorylation is induced within 30 min of cisplatin incubation, which is followed by p53 stabilization and accumulation in 2–4 h. The time course of p53 activation is consistent with its involvement in autophagy, which occurs within hours of cisplatin incubation. A previous study by Feng *et al.*[39] has suggested a regulation of autophagy by p53. Following activation, p53 can inactivate mammalian target of rapamycin via AMPK, leading to autophagy. Whether the same p53-signaling pathway mediates autophagy during cisplatin treatment of renal tubular cells, remains to be determined. Interestingly, our previous work has established a role for p53 in tubular cell apoptosis and renal injury induced by cisplatin.[17,18,36] Therefore, p53 can initiate the cell survival (autophagy) as well as the cell death (apoptosis)-signaling cascade. It is intriguing how the same molecule accomplishes two apparently opposite tasks and what determines the final outcome.

Another important autophagy regulator identified in this study is Bcl-2. Bcl-2 is well recognized as an antiapoptotic protein. However, stable expression of Bcl-2 can almost completely block the occurrence of autophagy during cisplatin incubation (Figure 5). The inhibitory effects of Bcl-2 are shown not only at early time points, but also at later time points of 24 h of cisplatin treatment (Figure 5). In previous studies, Bcl-2 has been proposed to inhibit autophagy by binding to Beclin-1. Bcl-2 binding of Beclin-1 may disrupt the protein complex (involving Beclin-1, UVRAG, vps15, and others) that is critical to vesicle nucleation, the start point of autophagosome formation.[40] While this is a tantalizing possibility, our preliminary experiments do not show a clear-cut Bcl-2/Beclin-1 interaction in co-immunoprecipitation assay (not shown). In addition to Beclin-1 binding, Bcl-2 may suppress autophagy by other indirect mechanisms. For example, the latest work by Hoyer-Hansen *et al.*[44] suggests that calcium release from endoplasmic reticulum during cell stress can activate Ca^{2+}/calmodulin-dependent kinases and AMPK, leading to inhibition of mammalian target of rapamycin and consequent activation of autophagy. Bcl-2 may suppress autophagy by diminishing calcium release in stressed cells. In line with this scenario, Bcl-2 localized to endoplasmic reticulum is inhibitory to autophagy, whereas mitochondrially targeted Bcl-2 inhibits only apoptosis but not autophagy.[44] Further investigations should test these interesting possibilities to gain insights into the autophagy regulation during cisplatin nephrotoxicity.

Functionally, our data suggest that autophagy is cytoprotective during cisplatin-induced renal cell injury. This conclusion is supported not only by the pharmacological experiments using 3-MA and BAF, but also by the Beclin-1 shRNA results. It is noteworthy that 3-MA and BAF block autophagy at up- and downstream levels, respectively.[42] 3-MA inhibits the autophagy-specific class-III phosphatidylinositol 3- kinase, which is crucial to vesicle nucleation or formation of pre-autophagasome, a very early event of autophagy. The same step is targeted by gene knockdown of Beclin-1. As a result, both 3-MA and Beclin-1 shRNA prevent punctate GFP-LC3 localization in autophagosome as well as LC3-II formation. In contrast, BAF inhibits fusion of lysosome with autophagosome, a late event in autophagy for final degradation of autophagocytosed materials. Thus, BAF does not prevent LC3 changes (Figure 6) in spite of its inhibitory effects on autophagy. What is important to recognize is that, regardless of the targeting steps (early or late) and approaches (pharmacological or genetic), inhibition of autophagy exacerbates apoptosis during cisplatin treatment (Figures 7 and 8). Certainly, such a conclusion needs to be further validated by *in vivo* studies using specific Atg-knockout models. The mechanism underlying pro-survival role of autophagy is largely unknown. Obviously, under conditions of starvation or nutrient deprivation, autophagy can prolong cell survival by self-digesting to sustain the basal energy demand of viability. In response to other types of stress, autophagy may remove or clean up the damaged macromolecules and subcellular organelles. In addition, we speculate that signaling activated during autophagy may interfere with cell death pathways. Further investigation

should focus on these possibilities to gain insights into the pathophysiological role of autophagy.

MATERIALS AND METHODS

Materials

RPTC, a rat kidney proximal tubular cell line, was originally obtained from Dr Hopfer (Case Western Reserve University, Cleveland, OH, USA). The cells were transfected with Bcl-2 to generate a stable Bcl-2-expressing cell line.[41] The cells were maintained and plated for experiments as described previously.[18] HEK cells were purchased from ATCC and maintained in minimal essential medium supplemented with 10% horse serum, glutamine, and antibiotics. C57BL/6 mice were purchased from Jackson Laboratory (Bar Harbor, ME, USA).

Antibodies were from the following sources: anti-LC3 from Dr Noboru Mizushima (Tokyo Metropolitan Institute of Medical Science, Tokyo, Japan), anti-Beclin-1 (Santa Cruz Biotechnology, Santa Cruz, CA, USA), anti-β-actin (Sigma, St Louis, MO, USA), secondary antibodies (Jackson ImmunoResearch, West Grove, PA, USA). PF was purchased from Calbiochem (San Diego, CA, USA). Other reagents, including cisplatin, 3-methyladenine, and BAF-A1, were from purchased from Sigma.

Models of cisplatin injury

For *in vitro* experiments, cisplatin was added to RPTCs or HEK cells in culture medium at the indicated concentrations as previously.[16–18] For *in vivo* experiments, male C57Bl/6 mice of 8–10 weeks were injected with a single dose (30 mg/kg body weight) of cisplatin as in our recent studies.[36,38] Renal function was monitored by measuring blood urea nitrogen and creatinine level. Renal tissues were collected at different time points for analysis. The animal protocol was approved by the Institutional Animal Care and Use Committees of Medical College of Georgia and VA Medical Center at Augusta.

Analysis of GFP-LC3 redistribution

The GFP-LC3 plasmid was a generous gift from Dr Yoshimori (National Institute of Genetics, Mishima, Japan) and was used recently to detect autophagy.[45] Transfection was conducted as detailed recently.[46] Briefly, cells were plated on a coverslip to reach ~50% confluence for transfection with 1 μg of plasmids by using Lipofectamine reagent (Invitrogen, Carlsbad, CA, USA). The cells were then maintained in culture medium for 24 h to reach 80–90% confluence for cisplatin treatment. At the end of incubation, cells were fixed with 4% paraformaldehyde and examined by fluorescence microscopy to count the cells with punctate GFP-LC3. Cell images were also collected by confocal microscopy as described.[46]

shRNA knockdown of Beclin-1

SureSilencing shRNA plasmids for Beclin-1 (Rat Becn1) were purchased from SuperArray (Frederick, MD, USA). A non-targeting shRNA was used as a control. Cells at ~50% confluence were transfected with various shRNA plasmids by using Lipofectamine 2000 reagent (Invitrogen). After transfection, cells were maintained in culture medium for 24 h to reach 80–90% confluence for cisplatin treatment or to collect whole-cell lysates for immunoblot analysis of Beclin-1.

Morphological examination of apoptosis

Apoptosis was evaluated by morphological criteria as described previously.[16,17,46] Typical apoptotic morphology included cellular shrinkage, nuclear condensation and fragmentation, and formation of apoptotic bodies. Briefly, at the end of the experiment, cells were stained with 10 μg/ml of Hoechst 33342. Cellular and nuclear morphology were then examined by phase-contrast and fluorescence microscopy. For cell count, four fields with ~200 cells per field were evaluated in each dish to estimate the percentage of cells with typical apoptotic morphology.

Immunoblot analysis

As described previously,[16,17,46] whole-cell or tissue lysates were homogenized in 2% SDS buffer. The same amounts of protein (usually 25 g, determined with the BCA reagent from Pierce Chemical (Rockford, IL, USA)) were loaded for each lane for reducing electrophoresis. The resolved proteins were then electro-blotted onto polyvinylidene difluoride membranes. The blots were incubated in a blocking buffer with 1% bovine serum albumin and 2% fat-free milk, and exposed to the primary antibodies overnight at 4 °C, and finally incubated with the horseradish peroxidase-conjugated secondary antibody to reveal antigens using an enhanced chemiluminescence kit from Pierce.

Electron microscopy

Renal tissues or cells were fixed at room temperature with a fixative containing 2.5% glutaraldehyde, 1% formaldehyde, 100 mM sodium phosphate, pH 7.2. The samples were then post-fixed in 1% osmium tetroxide, processed by standard procedures, and examined with a JEOL 1010 transmission electron microscope. In renal tissues, cells with high numbers of autophagic vacuoles or vesicles were counted in micrographs. In cultured cells, quantification of autophagic vesicles was performed as described previously.[45]

Statistics

Data were expressed as means ± s.d. ($n \geqslant 4$). Statistical differences between two groups were determined by Student's *t*-test with Microsoft EXCEL 2002. For comparison of multiple groups, analysis of variance with a *post hoc* test was conducted. $P < 0.05$ was considered to reflect significant differences.

DISCLOSURE

All the authors declared no competing interests.

ACKNOWLEDGMENTS

We thank Dr Tamotsu Yoshimori (National Institute of Genetics, Mishima, Japan) and Dr Noboru Mizushima (The Tokyo Metropolitan Institute of Medical Science, Tokyo, Japan) for the anti-LC3 antibody and GFP-LC3. This work was supported by grants from the National Institutes of Health and the US Department of Veterans Affairs. Part of the study was presented at the 2007 Annual Meeting of American Society of Nephrology.

REFERENCES

1. Klionsky DJ. Autophagy: from phenomenology to molecular understanding in less than a decade. *Nat Rev Mol Cell Biol* 2007; **8**: 931–937.
2. Levine B, Yuan J. Autophagy in cell death: an innocent convict? *J Clin Invest* 2005; **115**: 2679–2688.
3. Suzuki K, Ohsumi Y. Molecular machinery of autophagosome formation in yeast, *Saccharomyces cerevisiae*. *FEBS Lett* 2007; **581**: 2156–2161.
4. Shintani T, Klionsky DJ. Autophagy in health and disease: a double-edged sword. *Science* 2004; **306**: 990–995.
5. Liang XH, Jackson S, Seaman M *et al.* Induction of autophagy and inhibition of tumorigenesis by beclin 1. *Nature* 1999; **402**: 672–676.
6. Kabeya Y, Mizushima N, Ueno T *et al.* LC3, a mammalian homologue of yeast Apg8p, is localized in autophagosome membranes after processing. *EMBO J* 2000; **19**: 5720–5728.

7. Bonventre JV, Weinberg JM. Recent advances in the pathophysiology of ischemic acute renal failure. *J Am Soc Nephrol* 2003; **14**: 2199–2210.
8. Devarajan P. Update on mechanisms of ischemic acute kidney injury. *J Am Soc Nephrol* 2006; **17**: 1503–1520.
9. Molitoris BA, Sutton TA. Endothelial injury and dysfunction: role in the extension phase of acute renal failure. *Kidney Int* 2004; **66**: 496–499.
10. Vaidya VS, Ferguson MA, Bonventre JV. Biomarkers of acute kidney injury. *Annu Rev Pharmacol Toxicol* 2008; **48**: 463–493.
11. Goligorsky MS. Whispers and shouts in the pathogenesis of acute renal ischaemia. *Nephrol Dial Transplant* 2005; **20**: 261–266.
12. Arany I, Safirstein RL. Cisplatin nephrotoxicity. *Semin Nephrol* 2003; **23**: 460–464.
13. Pabla N, Dong Z. Cisplatin nephrotoxicity: mechanisms and renoprotective strategies. *Kidney Int* 2008; **73**: 994–1007.
14. Arany I, Megyesi JK, Kaneto H *et al.* Cisplatin-induced cell death is EGFR/src/ERK signaling dependent in mouse proximal tubule cells. *Am J Physiol Renal Physiol* 2004; **287**: F543–F549.
15. Cummings BS, Schnellmann RG. Cisplatin-induced renal cell apoptosis: caspase 3-dependent and -independent pathways. *J Pharmacol Exp Ther* 2002; **302**: 8–17.
16. Jiang M, Pabla N, Murphy RF *et al.* Nutlin-3 protects kidney cells during cisplatin therapy by suppressing Bax/Bak activation. *J Biol Chem* 2007; **282**: 2636–2645.
17. Jiang M, Wei Q, Wang J *et al.* Regulation of PUMA-alpha by p53 in cisplatin-induced renal cell apoptosis. *Oncogene* 2006; **25**: 4056–4066.
18. Jiang M, Yi X, Hsu S *et al.* Role of p53 in cisplatin-induced tubular cell apoptosis: dependence on p53 transcriptional activity. *Am J Physiol Renal Physiol* 2004; **287**: F1140–F1147.
19. Li S, Basnakian A, Bhatt R *et al.* PPAR-alpha ligand ameliorates acute renal failure by reducing cisplatin-induced increased expression of renal endonuclease G. *Am J Physiol Renal Physiol* 2004; **287**: F990–F998.
20. Lieberthal W, Triaca V, Levine J. Mechanisms of death induced by cisplatin in proximal tubular epithelial cells: apoptosis vs necrosis. *Am J Physiol* 1996; **270**: F700–F708.
21. Liu H, Baliga R. Cytochrome P450 2E1 null mice provide novel protection against cisplatin-induced nephrotoxicity and apoptosis. *Kidney Int* 2003; **63**: 1687–1696.
22. Nowak G. Protein kinase C-alpha and ERK1/2 mediate mitochondrial dysfunction, decreases in active Na+ transport, and cisplatin-induced apoptosis in renal cells. *J Biol Chem* 2002; **277**: 43377–43388.
23. Ramesh G, Reeves WB. TNFR2-mediated apoptosis and necrosis in cisplatin-induced acute renal failure. *Am J Physiol Renal Physiol* 2003; **285**: F610–F618.
24. Seth R, Yang C, Kaushal V *et al.* p53-Dependent caspase-2 activation in mitochondrial release of apoptosis-inducing factor and its role in renal tubular epithelial cell injury. *J Biol Chem* 2005; **280**: 31230–31239.
25. Shiraishi F, Curtis LM, Truong L *et al.* Heme oxygenase-1 gene ablation or expression modulates cisplatin-induced renal tubular apoptosis. *Am J Physiol Renal Physiol* 2000; **278**: F726–F736.
26. Yu F, Megyesi J, Safirstein RL *et al.* Identification of the functional domain of p21WAF1/CIP1 that protects from cisplatin cytotoxicity. *Am J Physiol Renal Physiol* 2005; **289**: F514–F520.
27. Ichimura T, Hung CC, Yang SA *et al.* Kidney injury molecule-1: a tissue and urinary biomarker for nephrotoxicant-induced renal injury. *Am J Physiol Renal Physiol* 2004; **286**: F552–F563.
28. Faubel S, Ljubanovic D, Reznikov L *et al.* Caspase-1-deficient mice are protected against cisplatin-induced apoptosis and acute tubular necrosis. *Kidney Int* 2004; **66**: 2202–2213.
29. Deng J, Kohda Y, Chiao H *et al.* Interleukin-10 inhibits ischemic and cisplatin-induced acute renal injury. *Kidney Int* 2001; **60**: 2118–2128.
30. Baek SM, Kwon CH, Kim JH *et al.* Differential roles of hydrogen peroxide and hydroxyl radical in cisplatin-induced cell death in renal proximal tubular epithelial cells. *J Lab Clin Med* 2003; **142**: 178–186.
31. Tanaka T, Kojima I, Ohse T *et al.* Hypoxia-inducible factor modulates tubular cell survival in cisplatin nephrotoxicity. *Am J Physiol Renal Physiol* 2005; **289**: F1123–F1133.
32. Zhou H, Kato A, Yasuda H *et al.* The induction of cell cycle regulatory and DNA repair proteins in cisplatin-induced acute renal failure. *Toxicol Appl Pharmacol* 2004; **200**: 111–120.
33. Pabla N, Huang S, Mi QS *et al.* ATR-Chk2 signaling in p53 activation and DNA damage response during cisplatin-induced apoptosis. *J Biol Chem* 2008; **283**: 6572–6583.
34. Bampton ET, Goemans CG, Niranjan D *et al.* The dynamics of autophagy visualized in live cells: from autophagosome formation to fusion with endo/lysosomes. *Autophagy* 2005; **1**: 23–36.
35. Mizushima N, Yoshimori T. How to interpret LC3 immunoblotting. *Autophagy* 2007; **3**: 542–545.
36. Wei Q, Dong G, Franklin J *et al.* The pathological role of Bax in cisplatin nephrotoxicity. *Kidney Int* 2007; **72**: 53–62.
37. Wei Q, Wang MH, Dong Z. Differential gender differences in ischemic and nephrotoxic acute renal failure. *Am J Nephrol* 2005; **25**: 491–499.
38. Wei Q, Dong G, Yang T *et al.* Activation and involvement of p53 in cisplatin-induced nephrotoxicity. *Am J Physiol Renal Physiol* 2007; **293**: F1282–F1291.
39. Feng Z, Zhang H, Levine AJ *et al.* The coordinate regulation of the p53 and mTOR pathways in cells. *Proc Natl Acad Sci USA* 2005; **102**: 8204–8209.
40. Pattingre S, Levine B. Bcl-2 inhibition of autophagy: a new route to cancer? *Cancer Res* 2006; **66**: 2885–2888.
41. Saikumar P, Dong Z, Patel Y *et al.* Role of hypoxia-induced Bax translocation and cytochrome *c* release in reoxygenation injury. *Oncogene* 1998; **17**: 3401–3415.
42. Maiuri MC, Zalckvar E, Kimchi A *et al.* Self-eating and self-killing: crosstalk between autophagy and apoptosis. *Nat Rev Mol Cell Biol* 2007; **8**: 741–752.
43. Jiang M, Wei Q, Pabla N *et al.* Effects of hydroxyl radical scavenging on cisplatin-induced p53 activation, tubular cell apoptosis and nephrotoxicity. *Biochem Pharmacol* 2007; **73**: 1499–1510.
44. Hoyer-Hansen M, Bastholm L, Szyniarowski P *et al.* Control of macroautophagy by calcium, calmodulin-dependent kinase kinase-beta, and Bcl-2. *Mol Cell* 2007; **25**: 193–205.
45. Ding WX, Ni HM, Gao W *et al.* Differential effects of endoplasmic reticulum stress-induced autophagy on cell survival. *J Biol Chem* 2007; **282**: 4702–4710.
46. Brooks C, Wei Q, Feng L *et al.* Bak regulates mitochondrial morphology and pathology during apoptosis by interacting with mitofusins. *Proc Natl Acad Sci USA* 2007; **104**: 11649–11654.